© 2013. Published by The Company of Biologists Ltd | Development (2013) 140, 4594-4601 doi:10.1242/dev.094078

RESEARCH ARTICLE

# Emilin3 is required for notochord sheath integrity and interacts with Scube2 to regulate notochord-derived Hedgehog signals

**Diana Corallo[1,*], Alvise Schiavinato[1,*], Valeria Trapani[1], Enrico Moro[1], Francesco Argenton[2] and Paolo Bonaldo[1,‡]**

## ABSTRACT

The notochord is a transient and essential structure that provides both mechanical and signaling cues to the developing vertebrate embryo. In teleosts, the notochord is composed of a core of large vacuolated cells and an outer layer of cells that secrete the notochord sheath. In this work, we have identified the extracellular matrix glycoprotein Emilin3 as a novel essential component of the zebrafish notochord sheath. The development of the notochord sheath is impaired in Emilin3 knockdown embryos. The patterning activity of the notochord is also affected by Emilin3, as revealed by the increase of Hedgehog (Hh) signaling in Emilin3-depleted embryos and the decreased Hh signaling in embryos overexpressing Emilin3 in the notochord. *In vitro* and *in vivo* experiments indicate that Emilin3 modulates the availability of Hh ligands by interacting with the permissive factor Scube2 in the notochord sheath. Overall, this study reveals a new role for an EMILIN protein and reinforces the concept that structure and function of the notochord are strictly linked.

**KEY WORDS: Extracellular matrix, EMILIN, Notochord, Hedgehog, Scube2, Zebrafish**

## INTRODUCTION

EMILINs (elastin microfibril interface located proteins) are extracellular matrix (ECM) glycoproteins belonging to the EMILIN/multimerin family. Emilin1, the founding member of this family, was originally identified as an ECM component associated with microfibrils in blood vessels (Bressan et al., 1993). Emilin3 contains the characteristic cysteine-rich EMI domain at the N-terminal end, followed by a region forming three coiled-coil structures at the C-terminal end (Schiavinato et al., 2012). At variance with the other EMILIN/multimerin proteins, Emilin3 is not expressed in the cardiovascular system and it lacks the C-terminal gC1q domain, which is involved in cell attachment and integrin binding (Spessotto et al., 2003; Danussi et al., 2011). Emilin3 expression during mouse development is particularly abundant in the perichondrium of developing bones (Leimeister et al., 2002; Doi et al., 2004; Schiavinato et al., 2012). We have previously found that eight EMILIN/multimerin genes are present in the zebrafish genome in four pairs of duplicated paralogs (Milanetto et al., 2008). Thus, Emilin3 is present in zebrafish with two genetic paralogs that we termed *emilin3a* and *emilin3b*. Similarly to the murine Emilin3 ortholog, the two zebrafish paralogs are not expressed in the cardiovascular system, whereas they are abundantly expressed in the notochord and in the chordoneural hinge until 24 hpf, and in cartilage primordia of the developing craniofacial skeleton at 48 hpf (Milanetto et al., 2008).

In the present study, we focused on the role of the two zebrafish Emilin3 genes during notochord development. During the early phases of embryonic development, until the segmentation stage, the notochord is distinguishable from adjacent tissues by the expression of specific genes, such as *shh*, *ehh* and *col2a1* (Yan et al., 1995; Currie and Ingham, 1996). As the notochord develops, expression of these early-transcribed genes is turned off and notochord cells differentiate in two different cell populations, an outer sheath layer and an inner vacuolated cell layer. The choice between these two fates is determined by Notch signals (Yamamoto et al., 2010). The outer cell layer is responsible for the synthesis of the notochord sheath, a thick peri-notochordal basement membrane that is composed of several ECM proteins, whereas the inner cells contain large intracellular vacuoles. Recently, the nature of these vacuoles was elegantly identified as lysosome-related organelles (Ellis et al., 2013). Both the notochord sheath and the vacuolated cells are essential for conferring the proper stiffness and rigidity to the notochord (Stemple, 2005).

Several studies in zebrafish showed that the formation of a notochord sheath is closely linked to the differentiation of notochord cells, and their reciprocal interactions are fundamental for the proper development and function of the notochord itself (Parsons et al., 2009; Pagnon-Minot et al., 2008; Mangos et al., 2010; Yamamoto et al., 2010). Here, we provide evidence that Emilin3 is a novel component of the notochord sheath that plays an essential role for the correct organization and the proper function of this structure. Moreover, we found that Emilin3 has a physiological role for limiting notochord-derived Hh signals, a function entailing the interaction of Emilin3 with the secreted protein Scube2.

## RESULTS

### Emilin3 is a novel essential component of the notochord sheath

To study Emilin3 protein distribution in the zebrafish embryo, we carried out whole-mount immunofluorescence with a polyclonal Emilin3 antibody. At 20 hpf, a specific signal was present throughout the notochord with a distinct posteroanterior gradient, whereas no labeling was detected in embryos at eight somites (data not shown; see also supplementary material Fig. S5D). At 24 hpf, Emilin3 became restricted to the notochord sheath, as confirmed by colocalization with collagen II. In agreement with mRNA expression data (Milanetto et al., 2008), labeling of the notochord sheath was lost at 48 hpf, indicating that Emilin3 undergoes a rapid turnover in the ECM and may fulfill a temporally restricted function during notochord development (Fig. 1A).

To investigate the role of Emilin3 during notochord development, we injected one- to two-cell-stage zebrafish embryos

[1]Department of Biomedical Sciences, University of Padova, I-35121 Padova, Italy.
[2]Department of Biology, University of Padova, I-35121 Padova, Italy.
*These authors contributed equally to this work

‡Author for correspondence (bonaldo@bio.unipd.it)

**Received 15 January 2013; Accepted 27 August 2013**

Development (2013) doi:10.1242/dev.094078

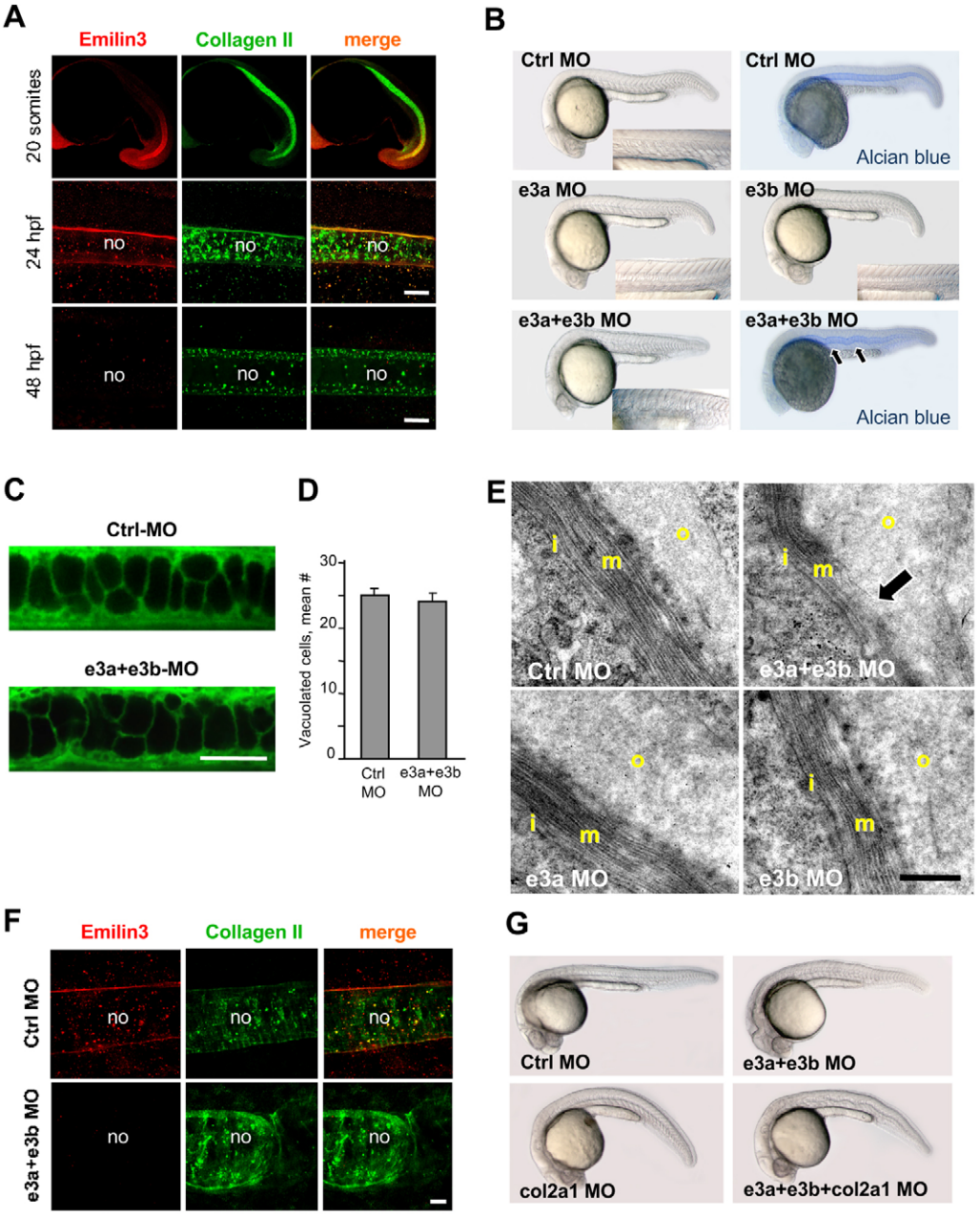


**Fig. 1. Emilin3 is an essential component of the notochord sheath.** (A) Lateral views of zebrafish embryos after immunofluorescence for Emilin3 and collagen II. Scale bars: 30 µm. (B) Lateral views of 24 hpf injected embryos. (C) BODIPY TR Ceramide staining of notochord cells in 24 hpf injected embryos. Scale bar: 50 µm. (D) Quantification of the mean number of vacuolated cells within the trunk region of control and treated notochord (not significantly different, $n$=10). Data are mean+s.e.m. (E) Transmission electron micrographs of the notochord sheath in transverse trunk sections of 30 hpf injected embryos. The arrow points at the medial layer of the notochord basement membrane, which is thinner and partially disorganized in Emilin3 double morphants. Scale bar: 500 nm. (F) Immunofluorescence for Emilin3 and collagen II in 24 hpf injected embryos. Scale bar: 10 µm. (G) Lateral views of 24 hpf injected embryos. col2a1 MO, *col2a1* morpholino; Ctrl MO, control morpholino; e3a MO, *emilin3a* morpholino; e3b MO, *emilin3b* morpholino; i, inner layer; m, medial layer; no, notochord; o, outer layer.

with antisense morpholino oligonucleotides targeting the splice sites between the first exon and the first intron of *emilin3a* and *emilin3b* genes. Co-injection of the two morpholinos resulted in the knockdown of the corresponding transcripts and proteins (supplementary material Fig. S1A,B), leading to a distinct distortion of the notochord with partial loss of the V-shaped conformation of somites and shortening of the main axis (Fig. 1B). Embryos injected with translation-blocking morpholinos for *emilin3a* and *emilin3b* showed a similar phenotype, and the same result was found in mixed experiments where a splice-blocking morpholino for one paralog was co-injected with a translation-blocking morpholino for the other paralog (supplementary material Fig. S1C; supplementary material Table S1). Injection of morpholinos targeting only one paralog did not cause a similar phenotype, even when injected at double concentration (Fig. 1B; supplementary material Table S1). As a further control, we performed p53 knockdown and found that co-injection of p53 morpholino was ineffective in rescuing the phenotypic defects induced by Emilin3 depletion (supplementary material Fig. S1D). Two different mechanisms could be inferred for the notochord phenotype of Emilin3 double morphants: (1) an increased pressure generated inside the notochord; or (2) a disruption of the sheath organization.

Quantification of total and vacuolated notochord cells in control and Emilin3 double morphant embryos did not reveal any significant difference, suggesting that Emilin3 deficiency is not grossly perturbing the morphology and commitment of notochord cells (Fig. 1C,D; supplementary material Fig. S2). Notch signaling is known to regulate the fate choice between vacuolated and non-vacuolated notochord cells (Yamamoto et al., 2010). Using the Tg_Hbb:EGFP Notch reporter zebrafish line (Parsons et al., 2009), we did not detect any major difference of Notch signaling activity in notochord cells of control and Emilin3 double morphant embryos (supplementary material Fig. S3).

Development (2013) doi:10.1242/dev.094078

We next investigated the structure of the notochord sheath by electron microscopy. At 30 hpf, in Emilin3 double morphants, but not in Emilin3 single morphants, the medial layer of the notochord basement membrane was not properly organized and many fibers appeared interrupted, whereas the outer and inner layers appeared normal (Fig. 1E). The medial and inner layers of the notochord sheath are thought to consist of collagen and laminin, respectively (Stemple, 2005). *In situ* hybridization and immunofluorescence showed that collagen II was more abundant in Emilin3-depleted embryos at both 24 and 48 hpf (Fig. 1F; supplementary material Fig. S4A,B), whereas laminin labeling was normal (supplementary material Fig. S4C). To exclude the possibility that the phenotype of Emilin3 morphants could be caused by an upregulation of collagen II, we performed concurrent knockdown of *emilin3a*, *emilin3b* and *col2a1*. Knockdown of *col2a1* caused ventral body curvature as expected (Mangos et al., 2010), whereas simultaneous knockdown of the three genes resulted in the overlap of the two phenotypes (Fig. 1G). Altogether, these data reveal that Emilin3 is essential for the normal structure of the notochord sheath.

### Emilin3 knockdown results in the upregulation of Hh signaling

Next, we investigated whether knockdown of Emilin3 could affect notochord patterning activity, a process that is largely mediated by the secretion of Hh ligands (Stemple, 2005). Expression of *ptc1* (*ptch2* – Zebrafish Information Network), which is transcriptionally regulated by Hh signaling (Concordet et al., 1996), was strongly increased in the trunk of 24 hpf Emilin3 morphants and this effect was completely blocked by treatment with 100 µM cyclopamine, an inhibitor of Hh signaling, but was unaffected by p53 (Tp53 – Zebrafish Information Network) knockdown (Fig. 2A; supplementary material Fig. S5A,B). To assess whether *ptc1* upregulation was specifically due to Emilin3 ablation, we analyzed *ptc1* expression at eight somites, a stage where Emilin3 proteins are not yet present in the sheath. Consistently, at this stage, *ptc1* was not differently expressed in Emilin3 morphants (supplementary material Fig. S5C,D).

Next, we generated the Tg12x_Gli zebrafish line, which express the mCherry reporter under the transcriptional regulation of Gli1 (see Materials and methods). We co-injected *emilin3a* and *emilin3b* morpholinos in Tg12x_Gli embryos and investigated expression of the transgene at 24 hpf. Notably, Emilin3 morphants displayed a remarkable increase of transgene expression (Fig. 2A), as also confirmed by qPCR experiments (Fig. 2B). We investigated the expression of other genes that respond to notochord-derived Hh signals in different embryonic structures. Expression of *nkx2.2a*, *tbx20* and *myoD1* was consistently increased in Emilin3-depleted embryos (Fig. 2C). Similarly, *olig2*, *vegf* and *eng2a* were upregulated (supplementary material Fig. S6A). Overexpression of Hh ligands by notochord cells can lead to hyperactivation of the Hh pathway (Yamamoto et al., 2010). At 20 somites, *shh* and *ehh*, the only two Hh ligands produced in the notochord, were not

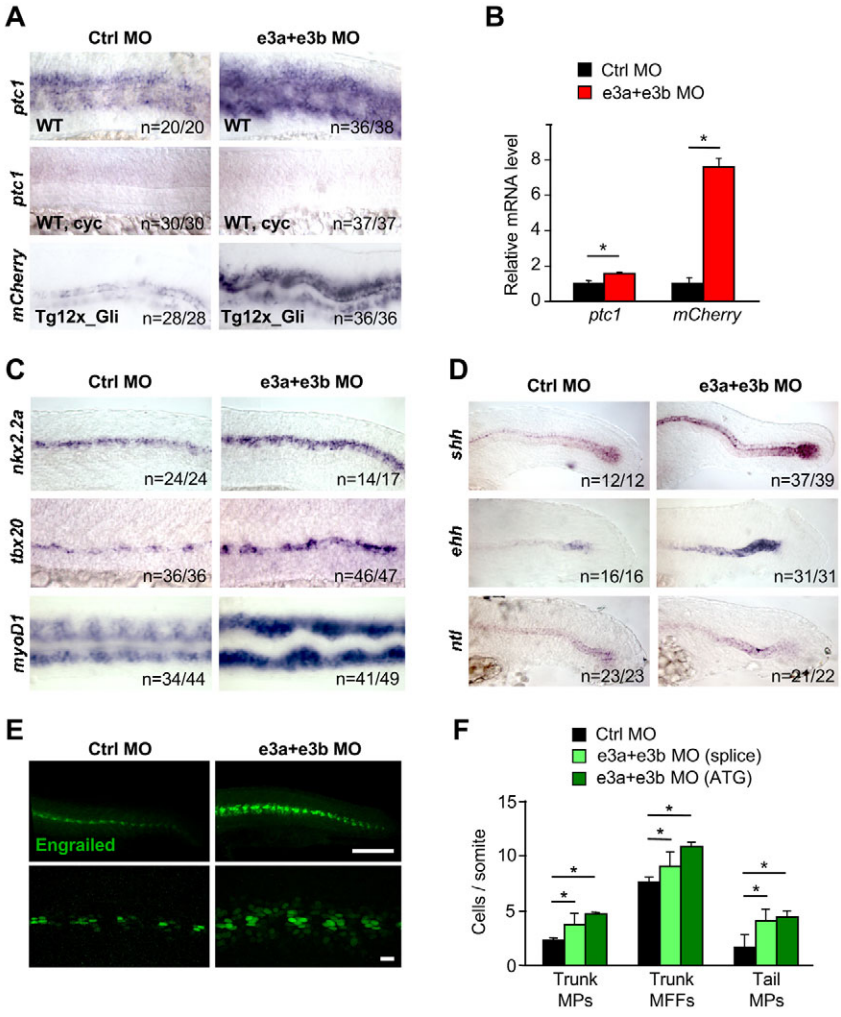


**Fig. 2. Hh signaling is upregulated in Emilin3 morphant embryos.** (A) Wild-type (WT) and Tg12x_Gli embryos were treated with 100 µM cyclopamine (cyc) and probed at 24 hpf by *in situ* hybridization for *ptc1* or *mCherry*. (B) qRT-PCR for *ptc1* and *mCherry* transcripts in Emilin3 morphant and control embryos (*$P$<0.05; $n$=30). (C) *In situ* hybridization for *nkx2.2a*, *tbx20* and *myoD1* in 24 hpf injected embryos. All images are lateral views, except for bottom panels (dorsal views). (D) *In situ* hybridization for *shh*, *ehh* and *ntl* in 24 hpf injected embryos. (E) Immunofluorescence for engrailed in 24 hpf injected embryos. Scale bars: 150 µm. (F) Quantification of engrailed-positive cells at 24 hpf (*$P$<0.05; $n$=10). Data are mean+s.e.m. Ctrl MO, control morpholino; e3a MO, *emilin3a* morpholino; e3b MO, *emilin3b* morpholino; e3a+e3b MO, *emilin3a* + *emilin3b* morpholinos; MPs, muscle pioneers; MFFs, medial fast fibers.

Development (2013) doi:10.1242/dev.094078

differently expressed in Emilin3 morphants when compared with control embryos (data not shown), whereas at 24 hpf they were upregulated in the distal part of the notochord (Fig. 2D). Therefore, the sole upregulation of *shh* and *ehh* did not explain the increased Hh activity in Emilin3 morphants. Moreover, expression of *ntl* and of the notochord-unrelated gene *fgf8* was not affected, thus excluding a developmental delay (Fig. 2D; supplementary material Fig. S6B).

We quantified engrailed-positive cells and found that both muscle pioneers (MPs) and medial fast fibers (MFFs) were significantly increased in Emilin3 morphants (Fig. 2E,F). It is known that engrailed expression in the zebrafish myotome is negatively regulated by BMP signaling (Du et al., 1997; Dolez et al., 2011), and high levels of Hh activity can prevent the accumulation of activated Smads in the medial part of the myotome (Maurya et al., 2011). Consistently, we found that expansion of the engrailed-positive domain in Emilin3 morphants was paralleled by a reduction of the pSmad1/5/8 domain in the medial part of the myotome. Treatment with low doses of cyclopamine was sufficient to rescue pSmad distribution in the somites of Emilin3 morphants, indicating that Hh pathway is primarily affected by Emilin3 knockdown (supplementary material Fig. S7A). To exclude the possibility that the observed effect on Hh signaling could be mediated by the pro-TGFβ inhibitory activity of Emilin3 (Schiavinato et al., 2012), we treated morphant embryos with two different selective inhibitors of TGFβ type I receptors, SB431542 and LY364947. Neither of these inhibitors was effective in decreasing *ptc1* expression, and pharmacological inhibition of TGFβ activity also exacerbated notochord distortion in Emilin3 morphants (supplementary material Fig. S7B).

### Emilin3 overexpression leads to downregulation of Hh target genes

To investigate whether upregulation of the Hh pathway was directly caused by Emilin3 deficiency or was a broader effect caused by disruption of the notochord sheath, we analyzed *ptc1* expression in *emilin3a* and *emilin3b* single morphants. Interestingly, albeit to a lesser extent than in Emilin3 double morphants, *ptc1* expression was increased in the trunk of single morphants (Fig. 3A). To further assess the role of Emilin3 in notochord-derived Hh signaling, we generated a pCS-twhh-mEmilin3 construct carrying murine full-length *Emilin3* cDNA under the control of a promoter that confers notochord-specific expression (Du et al., 1997). Embryos injected with this construct developed normally but at 24 hpf they displayed mild notochord defects and a shorter axis, when compared with embryos injected with a control pCS-twhh-β-gal construct (Fig. 3B). Notably, embryos injected with pCS-twhh-mEmilin3 showed impaired *myoD1* expression, together with reduced number of engrailed-positive cells. Emilin3 overexpression in the notochord did not influence *ehh* transcription, indicating that expression of Hh ligands by notochord cells was not grossly affected (Fig. 3B,C). Moreover, injection of the pCS-twhh-mEmilin3 construct also rescued the effects of morpholino-mediated ablation of Emilin3 both on notochord development and Hh signaling (supplementary material Fig. S8).

### Emilin3 functionally interacts with Scube2

As Emilin3 paralogs are expressed by notochord cells with a pattern closely similar to that of Hh ligands, we speculated that Emilin3 could influence the rate of synthesis and/or release of Hh proteins. Interestingly, when Emilin3 and Shh were transiently co-expressed in HEK293T cells, the amount of Shh released in media was

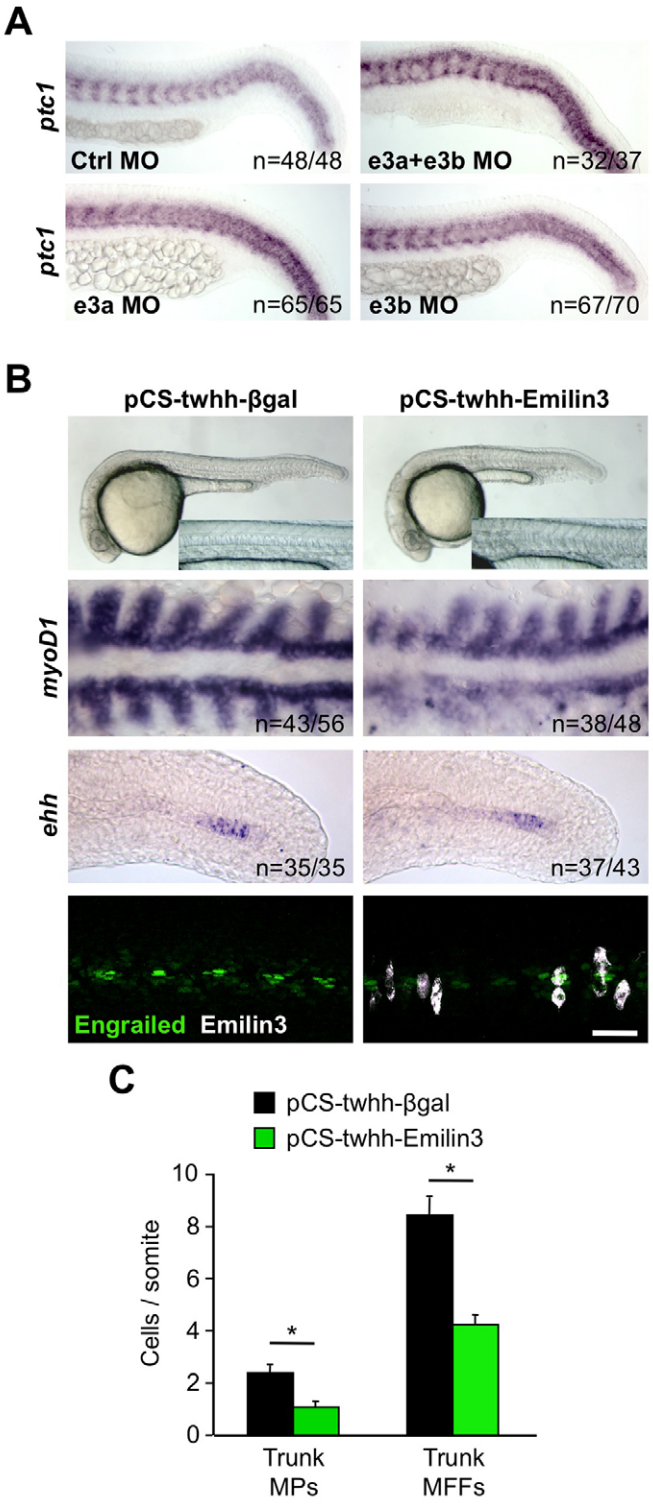


**Fig. 3. Overexpression of Emilin3 affects notochord patterning activity.** (A) Lateral views of 24 hpf embryos probed for *ptc1*. Embryos were injected with the indicated morpholinos. (B) Wild-type embryos were injected with the indicated constructs at 50 ng/µl and photographed at 24 hpf (upper panels), or probed by *in situ* hybridization for *myoD1* at eight somites and for *ehh* at 24 hpf (middle panels), or by immunofluorescence for engrailed and Emilin3 at 24 hpf (lower panels). Scale bar: 50 µm. (C) Quantification of engrailed-positive cells in 24 hpf embryos injected as in B (*$P$<0.05; $n$=15). Data are mean+s.e.m. Ctrl MO, control morpholino; e3a+e3b MO, *emilin3a* + *emilin3b* morpholinos; MPs, muscle pioneers; MFFs, medial fast fibers.

Development (2013) doi:10.1242/dev.094078

reduced (Fig. 4A). This effect was not dependent on the EMI domain and it was lost when Emilin3 was co-expressed with ShhN, a form of Shh lacking cholesterol modification (Fig. 4B,C). Co-immunoprecipitation experiments failed to reveal any interaction between Emilin3 and Shh (Fig. 4D). Therefore, we hypothesized that Emilin3 could interact with a factor secreted by HEK293T and involved in Shh release. To test this hypothesis, we used conditioned media derived from HEK293T transfected with empty vector or with Emilin3 construct to stimulate the release of Shh from stably transfected Shh-293 cells. Interestingly, the conditioned medium derived from mock-transfected cells strongly increased Shh release compared with fresh medium, whereas medium from Emilin3-transfected cells induced a much lower rate of Shh release (supplementary material Fig. S9).

Recent studies demonstrated a role for the secreted protein Scube2 in Shh release (Creanga et al., 2012; Tukachinsky et al., 2012). We therefore investigated whether Emilin3 could interact with Scube2. When HEK293T cells were co-transfected with Emilin3 and FLAG-tagged Scube2, Emilin3 was co-precipitated with Scube2 from media (Fig. 4E). Similarly, FLAG-tagged Scube2 was efficiently immunoprecipitated by HA-tagged Emilin3 (supplementary material Fig. S10A). This interaction was confirmed by *in vitro*-binding experiments and did not require the EMI domain or the coiled-coil region of Emilin3 (Fig. 4F,G). A similar *in vitro*-binding experiment showed that the EGF repeats of Scube2 are sufficient for Emilin3 binding (supplementary material Fig. S10B). To investigate whether the interaction of Emilin3 with Scube2 has any functional significance, we treated transfected HEK293T cells with conditioned media derived from Scube2-transfected cells. Notably, treatment with Scube2-conditioned media, as well as Scube2 co-transfection, were able to rescue the effect of Emilin3, whereas treatment with soluble heparin was ineffective (Fig. 4H; supplementary material Fig. S10C-E). We also prepared conditioned media derived from HEK293T transiently transfected with Scube2 alone or in combination with Emilin3, and found that the latter was less effective in releasing Shh from 293-Shh cells (Fig. 4I).

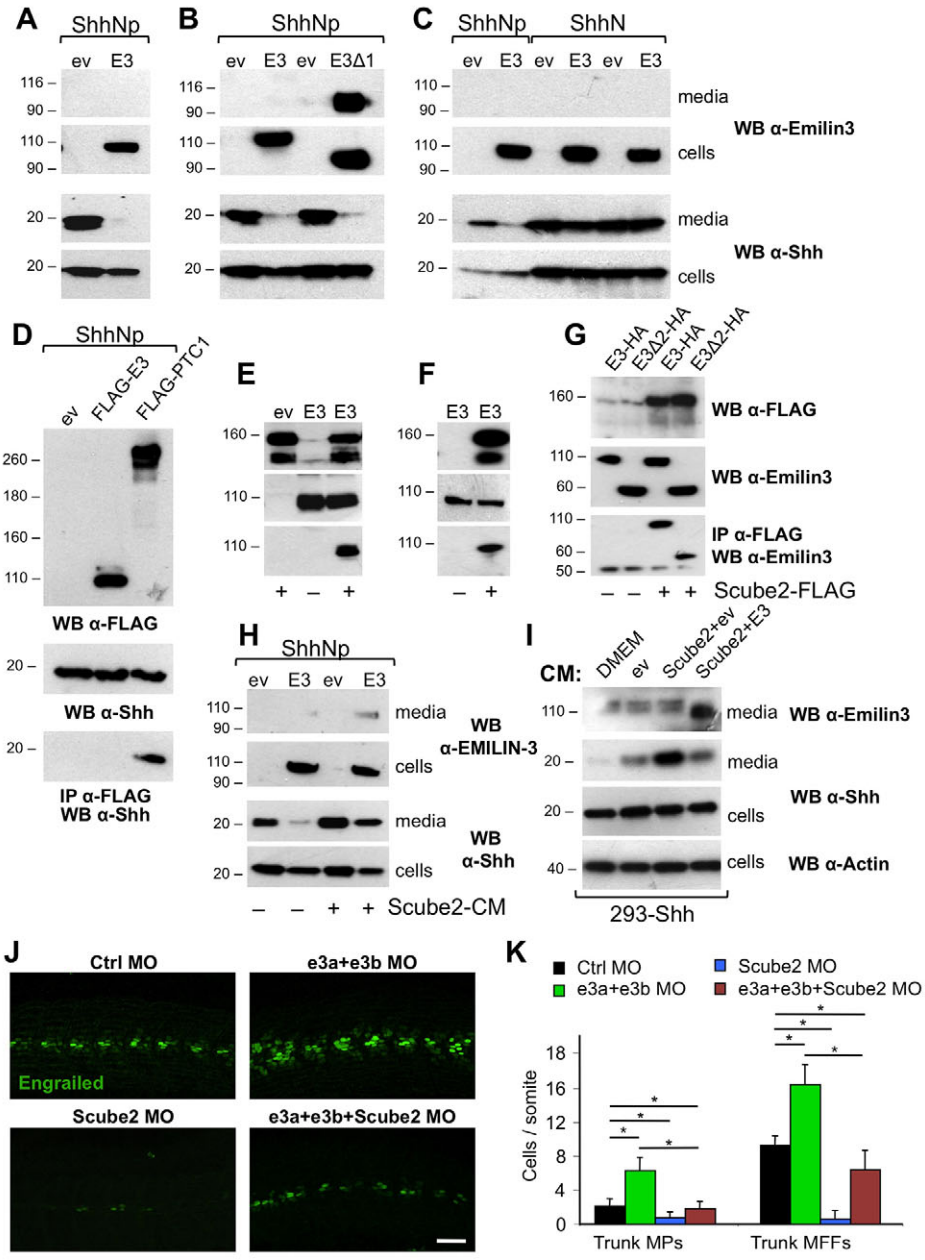


**Fig. 4. Emilin3 functionally interacts with Scube2**. (A-C) HEK293T were transiently co-transfected with the indicated constructs. Conditioned serum-free media and cell lysates were analyzed by western blot. (D) Cell lysates of HEK293T transfected with the indicated plasmids were analyzed by western blot or subjected to immunoprecipitation. (E-G) HEK293T were either co-transfected (E,G) or separately transfected (F) with the indicated plasmids. Media (E,F) and cell lysates (G) were analyzed by western blot or subjected to immunoprecipitation. (H) Transfected HEK293T were incubated for 24 hours with conditioned media derived from control or Scube2-transfected cells. (I) Stably transfected 293-Shh cells were incubated for 6 hours with fresh medium (DMEM) or with conditioned media derived from HEK293T co-transfected with the indicated plasmids. Media and cell lysates were analyzed by western blot. (J) Lateral views of 24 hpf embryos injected with the indicated morpholinos and immunostained for engrailed. Scale bar: 50 μm. (K) Quantification of engrailed-positive cells in injected embryos (*$P$<0.05; $n$=6). Data are mean+s.e.m. CM, conditioned media; E3, murine full-length Emilin3; E3Δ1, murine Emilin3 lacking the EMI domain; E3Δ2, murine Emilin3 lacking the EMI domain and the coiled-coil region; ev, empty vector; IP, immunoprecipitation; PTC1, human FLAG-patched-1; WB, western blot; Ctrl MO, control morpholino; e3a+e3b MO, *emilin3a* + *emilin3b* morpholinos; Scube2 MO, Scube2 morpholino; MPs, muscle pioneers; MFFs, medial fast fibers.

Development (2013) doi:10.1242/dev.094078

Finally, to investigate whether the interaction of Emilin3 with Scube2 was relevant *in vivo*, we injected embryos with morpholinos directed against *emilin3a*/*emilin3b* and *scube2*, as well as their combination. Emilin3 knockdown resulted in a robust increase of both MFFs and MPs, whereas Scube2 morphants lacked engrailed-positive cells as expected (Woods and Talbot, 2005). Interestingly, although co-injection of the three morpholinos resulted in the overlap of the two phenotypes (supplementary material Fig. S11A), the number of engrailed-positive cells was rescued almost to wild-type levels in triple morphants (Fig. 4J,K). qRT-PCR experiments showed that Scube2 expression was slightly, albeit not significantly, upregulated in Emilin3-depleted embryos (supplementary material Fig. S11B). Overall, these results support a physiological role for Emilin3 in limiting the activity of Scube2 on the release of Hh ligands by notochord cells.

## DISCUSSION

In this work, we provided the first *in vivo* functional characterization of Emilin3, revealing both structural and functional roles for notochord development in zebrafish. Electron microscopy showed that Emilin3 is required for proper structural organization of the peri-notochordal basement membrane. In the absence of Emilin3, the sheath is not resistant enough to withstand the pressure generated by vacuolization of notochord cells, and this defect provides an explanation for the notochord distortion we observed in Emilin3 morphants.

Interestingly, the notochord phenotype of Emilin3 double morphant embryos is similar to that described for other ECM components. In particular, the ultrastructural alterations we found in the medial layer of the notochord sheath are reminiscent of those described for the zebrafish *gulliver* mutants, which carry a missense mutation in the globular C1q domain of the *col8a1* gene (Gansner and Gitlin, 2008). Intriguingly, unlike other EMILIN proteins, this domain is missing in Emilin3. It has been shown that the globular C1q domain is involved in the supramolecular organization of EMILINs by interacting with the EMI domain (Doliana et al., 2000), thus suggesting the possibility that Emilin3 and collagen VIII are interacting partners in the medial layer of the notochord sheath.

Our data also support previous findings, which indicated that defects in the notochord sheath can influence the gene expression pattern of notochord cells. However, at odds with what is observed in other models of notochord disruption (Parsons et al., 2002; Pagnon-Minot et al., 2008; Yamamoto et al., 2010), we found that *col2a1* and Hh ligands are not co-regulated. Indeed, in Emilin3 double morphants, *col2a1* expression is upregulated throughout the length of the notochord, whereas *shh* and *ehh* are overexpressed only in the expression field of *emilin3a* and *emilin3b*, at the level of the chordoneural hinge. Conversely, laminin mutants and collagen XV morphants display a similar upregulation of *col2a1* and *ehh* throughout the notochord (Parsons et al., 2002; Pagnon-Minot et al., 2008). This implies that notochord cells can respond to extracellular signals in a region-specific way.

The second function we report here for Emilin3 concerns the regulation of notochord-derived Hh signals. We show that Emilin3 interacts with Scube2 in the extracellular environment. Recently, Scube2 has been identified as a secreted, permissive factor, acting non-cell autonomously in the release of lipidated Shh from producing cells (Creanga et al., 2012; Tukachinsky et al., 2012). Scube2 is a multi-domain protein, with a signal peptide sequence at the N-terminal end followed by nine EGF repeats, one spacer region, three cysteine-rich motifs and one CUB domain at the C-terminal end. The CUB domain was found to interact with Shh and its presence is required for the activity of Scube2 on Shh release (Creanga et al., 2012; Tukachinsky et al., 2012). Our finding that Emilin3 is able to interact with the EGF repeats of Scube2 supports the hypothesis that this region of the protein may be important for targeting Scube2 to the ECM and fine-tuning its localization and activity in the extracellular milieu. We therefore propose that Emilin3 deficiency disturbs notochord sheath formation and causes abnormal localization and/or activity of Scube2 in the extracellular milieu, thus leading to increased Hh signals (Fig. 5). It is tempting to speculate that Emilin3, similar to Emilin1, associates with fibrillin microfibrils in the ECM, and thus the Scube2/Emilin3 interaction may represent a novel mechanism by which microfibrils control tissues homeostasis. Overall, our data indicate that the ECM endows a novel level of regulation for Hh signals through Scube2, and we propose that Emilin3 and Scube2 interaction in the notochord sheath is crucial for the proper notochord patterning activity.

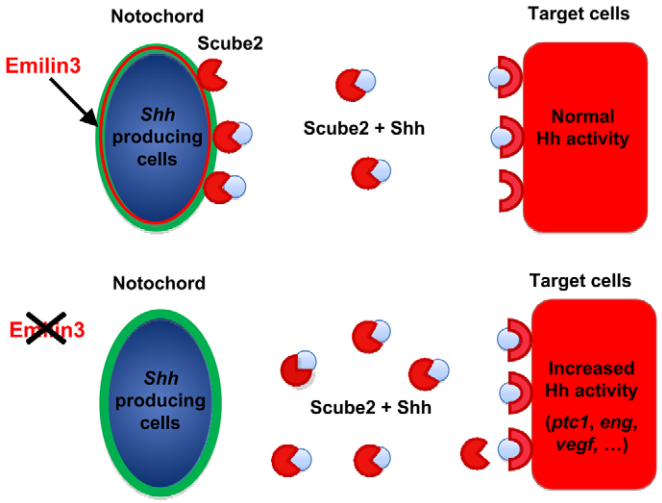


**Fig. 5. Hypothetical model of Emilin3 and Scube2 interaction in the notochord sheath.** Emilin3 is located in the extracellular matrix of the notochord sheath and interacts with Scube2, a secreted factor that mediates the release of lipid-modified Hh ligand. In wild-type embryos, Emilin3 ensures the integrity and function of the notochord sheath, which is necessary for proper notochord patterning activity. Emilin3 deficiency results in the disruption of the notochord sheath and affects Scube2 localization and activity in the extracellular milieu, thus leading to increased Hh signals.

## MATERIALS AND METHODS

### Zebrafish lines

Wild-type (AB/TU) zebrafish were maintained as described previously (Westerfield, 1995). For the generation of the *Tg(12xGli-HSVTK:nlsmCherry)ia10* zebrafish line (Tg12x_Gli), a cassette containing twelve multimerized Gli1-binding sites was isolated from the 12GLI-RE-TKO-luc construct (Kogerman et al., 1999) and ligated with the Herpes simplex virus thymidine kinase minimal promoter in the p5E-MCS Tol2 5′ entry vector. Positive clones were sequenced in both strands and recombined with a middle entry vector carrying the *mCherry* open reading frame and a 3′ entry vector carrying a SV40 poly-A tail. Entry plasmids were finally recombined into the pTol2 destination vector as previously described (Kwan et al., 2007). A total of 25 pg of Tol2 recombinant plasmids and 25-50 pg of *in vitro* synthesized transposase mRNA (Kawakami et al., 2004) were co-injected into zebrafish embryos at the one- to two-cell stage. Microinjected embryos were raised to adulthood and outcrossed to wild-type fish. Six out of 30 screened fish were identified as founders for the reporter line. The *Tg(EPV.TP1-Mmu.Hbb:EGFP)ia12* zebrafish line (Tg_Hbb:EGFP) has been previously described (Parsons et al., 2009).

### Zebrafish embryo injection

Sequences of the morpholinos used in the study are reported in supplementary material Table S2. All morpholinos were splice blocked, except where indicated. Morpholinos were dissolved in 1×Danieu's buffer and injected at the doses reported in supplementary material Table S1. p53 morpholino (Robu et al., 2007) and Scube2 morpholino (Woods and Talbot, 2005) were injected at 6 ng/embryo and 2 ng/embryo, respectively. For DNA microinjection, linearized DNA was dissolved in deionised $H_2O$ to a final concentration of at 50 ng/µl (Du et al., 1997), except where indicated. Murine *Emilin3* cDNA was cloned into the pCS-twhh-βgal vector (Du et al., 1997).

### Pharmacological treatments

Cyclopamine hydrate (Sigma) was dissolved in DMSO and embryos were incubated at the indicated concentrations beginning at shield stage until fixation at 24 hpf. LY364947 (Zhou et al., 2011) and SB431542 (Ho et al., 2006) (Sigma) were dissolved in DMSO and diluted into embryo medium to a final concentration of 30 µM and 100 µM, respectively, and embryos were incubated with these compounds from 8 hpf until fixation at 24 hpf. Embryos incubated with DMSO were used as control.

### Probes and plasmids

For *in situ* hybridization experiments, the used riboprobes were: *emilin3a* and *emilin3b* (Milanetto et al., 2008), *col2a1* (Yan et al., 1995), *ntl* (Schulte-Merker et al., 1994), *shh* (Krauss et al., 1993), *ehh* (Currie and Ingham, 1996), *ptc1* (Concordet et al., 1996), *nkx2.2a* (Barth and Wilson, 1995), *tbx20* (Ahn et al., 2000), *vegf* (Liang et al., 1998), *olig2* (Park et al., 2002), *eng2a* (Ekker et al., 1992), and *fgf8* (Reifers et al., 1998). The cDNA constructs for murine full-length Emilin3 and EMILIN-3Δ1, which lacks amino acid residues 54-189, have been described previously (Schiavinato et al., 2012). Murine EMILIN-3Δ2 cDNA construct, which lacks both the EMI domain (amino acid residues 54-189) and the coiled-coil region (amino acid residues 534-758), was prepared by PCR using the EMILIN-3Δ1 construct as a template and the following primers: SP6 (forward) and 5′-CTAAGCGTAATCTGGAACATCGTATGGGTACCAGGCCTTCACCTC-TGC-3′ (reverse). The EMILIN-3-HA cDNA construct was generated by adding the human influenza hemagglutinin (HA) tag sequence at the C-terminal end of murine full-length Emilin3. Murine full-length Shh, ShhN and Scube2 cDNAs were obtained by PCR and cloned into the pCS2+ vector. The Scube2-FLAG construct was generated by adding the FLAG tag sequence at the C-terminal end of murine Scube2. The EGF-FLAG construct, encompassing amino acids 1-479 of murine Scube2, was generated by PCR using the Scube2 full-length construct as a template with the following primers: 5′-GGTTGCATGCTGATGGGAGA-3′ (forward) and 5′-TTCTCGAGTCACTTGTCATCGTCGTCCTTGTAGTCTGACGAGA-GGTGAATGCC-3′ (reverse, coding for the FLAG tag sequence). The PCR product was then subcloned into the pCS2 vector. All constructs were sequenced prior to use.

### Immunohistochemistry and BODIPY labeling

Immunohistochemical staining of whole zebrafish embryos was performed essentially as described previously (Dolez et al., 2011). Used antibodies were: monoclonal anti-engrailed (4D9, DSHB; 1:10 dilution); monoclonal anti-collagen II (II-II6B3, DSHB; 1:400); rabbit polyclonal anti-laminin (L9393, Sigma; 1:200); rabbit polyclonal anti-phospho-Smad1/Smad5/Smad8 (9511, Cell Signaling; 1:100); rabbit polyclonal anti-Emilin3 (Schiavinato et al., 2012; 1:500); mouse monoclonal anti-β-Catenin (C7207, Sigma; 1:500). Nuclei were stained with Hoechst (Invitrogen). Where indicated, embryos were stained with 100 µM BODIPY TR Ceramide (Invitrogen) in E3 medium for 2 hours. All embryos were imaged with a Leica SP5 confocal microscope.

### Electron microscopy

Embryos were prepared essentially as described previously (Parsons, 2002) and ultrathin sections were viewed on a Zeiss 902 electron microscope.

### RNA analysis

Total RNA was extracted from pools of 30 embryos using TRIzol Reagent (Invitrogen) as recommended by the manufacturer and 1 µg of RNA was used for cDNA synthesis, using the M-MLV Reverse Transcriptase kit (Invitrogen). The efficacy of splice-blocking morpholinos was tested by RT-PCR using the following primers: 5′-ACGTGCTGAAATTGGTGGA-3′ (*emilin3a*, forward); 5′-GGAACAGCTTGACCTTCGAG-3′ (*emilin3a*, reverse); 5′-ACTCAAGCAAGCTGGACCAT-3′ (*emilin3b*, forward); 5′-CCTTGTGTGTGGAGCGACA-3′ (*emilin3b*, reverse). Expression of *nlsmCherry*, *ptc1* and *scube2* transcripts was analyzed by real-time qualitative RT-PCR using the SYBR Green Realtime PCR Master Mix in an ABI PRISM 7900HT System (Applied Biosystems). Expression of *gapdh* was used as normalizer in each sample and triplicate PCR reactions were carried out. Primers used were: 5′-GTGGAGTCTACTGGTGTCTTC-3′ (*gapdh*, forward); 5′-GTGCAGGAGGCATTGCTTACA-3′ (*gapdh*, reverse); 5′-GAAGGTGACCAAGGGCGGCC-3′ (*nlsmCherry*, forward); 5′-CTGGGTCACGGTCACCACGC-3′ (*nlsmCherry*, reverse); 5′-CTTCAGTCGCCAAGGTCTTC-3′ (*ptc1*, forward); 5′-CCGATCAATCC-CATCATACC-3′ (*ptc1*, reverse); 5′-GCAAGGCTTTTTCCTGAGTG-3′ (*scube2*, forward); 5′-TTACCATGGTTGCAGGTCAA-3′ (*scube2*, reverse).

### Cell culture and transfection

HEK293T were grown in DMEM supplemented with 10% FBS (Invitrogen) and transfected with LT-1 (Mirus). The next day cells were washed and incubated in serum-free medium. For the preparation of Scube2-conditioned medium, cells were transfected and kept in DMEM supplemented with 2% FBS for 72 hours. Stably transfected HEK-293 (293-Shh) cells were generated by transfection with the murine full-length Shh cDNA subcloned into the pcDNA3.1+ vector, followed by selection with G418 (Invitrogen) at a concentration of 400 µg/ml.

### Western blot and immunoprecipitation

Cells and conditioned media were harvested 24 hours (western blot) or 72 hours (immunoprecipitation) after incubation in serum-free medium. Cells were lysed in ice-cold lysis buffer [25 mM Tris (pH 7.5), 150 mM NaCl, 2.5 mM EDTA, 10% glycerol, 1% Nonidet P-40] supplemented with proteases inhibitor (Roche) and media were TCA precipitated. Immunoprecipitation, SDS-PAGE and western blot were performed as previously described (Schiavinato et al., 2012). Used antibodies were: rabbit polyclonal anti-Emilin3 (Schiavinato et al., 2012), rabbit polyclonal anti-Shh (Santa Cruz), mouse monoclonal anti-FLAG (Sigma) and mouse monoclonal anti-HA (Sigma).

### Statistical analysis

Data are expressed as mean±s.e.m. Statistical significance was determined by unequal variance Student's *t*-test. $P<0.05$ was considered significant.

#### Acknowledgements

We thank Walter Giuriati for help with electron microscopy. We are grateful to Professor Mats Paulsson and Dr Raimund Wagener for Emilin3 antibody and for critical reading of the manuscript.

#### Competing interests

The authors declare no competing financial interests.

#### Author contributions

D.C. and A.S. conceived and performed the majority of the experiments, and analyzed data. V.T. performed experiments and analyzed data. E.M. and F.A. provided zebrafish transgenic lines, contributed new reagents/analytic tools. P.B. and A.S. designed the study, analyzed data and wrote the paper. All authors discussed the results and commented on the manuscript.

#### Funding

This work was supported by grants from the University of Padova and the Italian Ministry of University and Research.

#### Supplementary material

Supplementary material available online at
http://dev.biologists.org/lookup/suppl/doi:10.1242/dev.094078/-/DC1

## References


**Ahn, D. G., Ruvinsky, I., Oates, A. C., Silver, L. M. and Ho, R. K.** (2000). tbx20, a new vertebrate T-box gene expressed in the cranial motor neurons and developing cardiovascular structures in zebrafish. *Mech. Dev.* **95**, 253-258.

**Barth, K. A. and Wilson, S. W.** (1995). Expression of zebrafish nk2.2 is influenced by sonic hedgehog/vertebrate hedgehog-1 and demarcates a zone of neuronal differentiation in the embryonic forebrain. *Development* **121**, 1755-1768.

**Bressan, G. M., Daga-Gordini, D., Colombatti, A., Castellani, I., Marigo, V. and Volpin, D.** (1993). Emilin, a component of elastic fibers preferentially located at the elastin-microfibrils interface. *J. Cell Biol.* **121**, 201-212.

**Concordet, J. P., Lewis, K. E., Moore, J. W., Goodrich, L. V., Johnson, R. L., Scott, M. P. and Ingham, P. W.** (1996). Spatial regulation of a zebrafish patched homologue reflects the roles of sonic hedgehog and protein kinase A in neural tube and somite patterning. *Development* **122**, 2835-2846.

**Creanga, A., Glenn, T. D., Mann, R. K., Saunders, A. M., Talbot, W. S. and Beachy, P. A.** (2012). Scube/You activity mediates release of dually lipid-modified Hedgehog signal in soluble form. *Genes Dev.* **26**, 1312-1325.

**Currie, P. D. and Ingham, P. W.** (1996). Induction of a specific muscle cell type by a hedgehog-like protein in zebrafish. *Nature* **382**, 452-455.

**Danussi, C., Petrucco, A., Wassermann, B., Pivetta, E., Modica, T. M., Del Bel Belluz, L., Colombatti, A. and Spessotto, P.** (2011). EMILIN1-α4/α9 integrin interaction inhibits dermal fibroblast and keratinocyte proliferation. *J. Cell Biol.* **195**, 131-145.

**Doi, M., Nagano, A. and Nakamura, Y.** (2004). Molecular cloning and characterization of a novel gene, EMILIN-5, and its possible involvement in skeletal development. *Biochem. Biophys. Res. Commun.* **313**, 888-893.

**Dolez, M., Nicolas, J. F. and Hirsinger, E.** (2011). Laminins, via heparan sulfate proteoglycans, participate in zebrafish myotome morphogenesis by modulating the pattern of Bmp responsiveness. *Development* **138**, 97-106.

**Doliana, R., Bot, S., Bonaldo, P. and Colombatti, A.** (2000). EMI, a novel cysteine-rich domain of EMILINs and other extracellular proteins, interacts with the gC1q domains and participates in multimerization. *FEBS Lett.* **484**, 164-168.

**Du, S. J., Devoto, S. H., Westerfield, M. and Moon, R. T.** (1997). Positive and negative regulation of muscle cell identity by members of the hedgehog and TGF-beta gene families. *J. Cell Biol.* **139**, 145-156.

**Ekker, M., Wegner, J., Akimenko, M. A. and Westerfield, M.** (1992). Coordinate embryonic expression of three zebrafish engrailed genes. *Development* **116**, 1001-1010.

**Ellis, K., Bagwell, J. and Bagnat, M.** (2013). Notochord vacuoles are lysosome-related organelles that function in axis and spine morphogenesis. *J. Cell Biol.* **200**, 667-679.

**Gansner, J. M. and Gitlin, J. D.** (2008). Essential role for the alpha 1 chain of type VIII collagen in zebrafish notochord formation. *Dev. Dyn.* **237**, 3715-3726.

**Ho, D. M., Chan, J., Bayliss, P. and Whitman, M.** (2006). Inhibitor-resistant type I receptors reveal specific requirements for TGF-beta signaling in vivo. *Dev. Biol.* **295**, 730-742.

**Kawakami, K.** (2004). Transgenesis and gene trap methods in zebrafish by using the Tol2 transposable element. *Methods Cell Biol.* **77**, 201-222.

**Kogerman, P., Grimm, T., Kogerman, L., Krause, D., Undén, A. B., Sandstedt, B., Toftgård, R. and Zaphiropoulos, P. G.** (1999). Mammalian suppressor-of-fused modulates nuclear-cytoplasmic shuttling of Gli-1. *Nat. Cell Biol.* **1**, 312-319.

**Krauss, S., Concordet, J. P. and Ingham, P. W.** (1993). A functionally conserved homolog of the Drosophila segment polarity gene hh is expressed in tissues with polarizing activity in zebrafish embryos. *Cell* **75**, 1431-1444.

**Kwan, K. M., Fujimoto, E., Grabher, C., Mangum, B. D., Hardy, M. E., Campbell, D. S., Parant, J. M., Yost, H. J., Kanki, J. P. and Chien, C. B.** (2007). The Tol2kit: a multisite gateway-based construction kit for Tol2 transposon transgenesis constructs. *Dev. Dyn.* **236**, 3088-3099.

**Leimeister, C., Steidl, C., Schumacher, N., Erhard, S. and Gessler, M.** (2002). Developmental expression and biochemical characterization of Emu family members. *Dev. Biol.* **249**, 204-218.

**Liang, D., Xu, X., Chin, A. J., Balasubramaniyan, N. V., Teo, M. A. L., Lam, T. J., Weinberg, E. S. and Ge, R.** (1998). Cloning and characterization of vascular endothelial growth factor (VEGF) from zebrafish, *Danio rerio*. *Biochim. Biophys. Acta* **1397**, 14-20.

**Mangos, S., Lam, P. Y., Zhao, A., Liu, Y., Mudumana, S., Vasilyev, A., Liu, A. and Drummond, I. A.** (2010). The ADPKD genes pkd1a/b and pkd2 regulate extracellular matrix formation. *Dis. Model. Mech.* **3**, 354-365.

**Maurya, A. K., Tan, H., Souren, M., Wang, X., Wittbrodt, J. and Ingham, P. W.** (2011). Integration of Hedgehog and BMP signalling by the engrailed2a gene in the zebrafish myotome. *Development* **138**, 755-765.

**Milanetto, M., Tiso, N., Braghetta, P., Volpin, D., Argenton, F. and Bonaldo, P.** (2008). Emilin genes are duplicated and dynamically expressed during zebrafish embryonic development. *Dev. Dyn.* **237**, 222-232.

**Pagnon-Minot, A., Malbouyres, M., Haftek-Terreau, Z., Kim, H. R., Sasaki, T., Thisse, C., Thisse, B., Ingham, P. W., Ruggiero, F. and Le Guellec, D.** (2008). Collagen XV, a novel factor in zebrafish notochord differentiation and muscle development. *Dev. Biol.* **316**, 21-35.

**Park, H. C., Mehta, A., Richardson, J. S. and Appel, B.** (2002). olig2 is required for zebrafish primary motor neuron and oligodendrocyte development. *Dev. Biol.* **248**, 356-368.

**Parsons, M. J., Pollard, S. M., Saude, L., Feldman, B., Coutinho, P., Hirst, E. M. and Stemple, D. L.** (2002). Zebrafish mutants identify an essential role for laminins in notochord formation. *Development* **129**, 3137-3146.

**Parsons, M. J., Pisharath, H., Yusuff, S., Moore, J. C., Siekmann, A. F., Lawson, N. and Leach, S. D.** (2009). Notch-responsive cells initiate the secondary transition in larval zebrafish pancreas. *Mech. Dev.* **126**, 898-912.

**Reifers, F., Böhli, H., Walsh, E. C., Crossley, P. H., Stainier, D. Y. R. and Brand, M.** (1998). *Fgf8* is mutated in zebrafish acerebellar (ace) mutants and is required for maintenance of midbrain-hindbrain boundary development and somitogenesis. *Development* **125**, 2381-2395.

**Robu, M. E., Larson, J. D., Nasevicius, A., Beiraghi, S., Brenner, C., Farber, S. A. and Ekker, S. C.** (2007). p53 activation by knockdown technologies. *PLoS Genet.* **3**, e78.

**Schiavinato, A., Becker, A. K., Zanetti, M., Corallo, D., Milanetto, M., Bizzotto, D., Bressan, G., Guljelmovic, M., Paulsson, M., Wagener, R. et al.** (2012). EMILIN-3, peculiar member of elastin microfibril interface-located protein (EMILIN) family, has distinct expression pattern, forms oligomeric assemblies, and serves as transforming growth factor β (TGF-β) antagonist. *J. Biol. Chem.* **287**, 11498-11515.

**Schulte-Merker, S., Hammerschmidt, M., Beuchle, D., Cho, K. W., De Robertis, E. M. and Nüsslein-Volhard, C.** (1994). Expression of zebrafish goosecoid and no tail gene products in wild-type and mutant no tail embryos. *Development* **120**, 843-852.

**Spessotto, P., Cervi, M., Mucignat, M. T., Mungiguerra, G., Sartoretto, I., Doliana, R. and Colombatti, A.** (2003). beta 1 Integrin-dependent cell adhesion to EMILIN-1 is mediated by the gC1q domain. *J. Biol. Chem.* **278**, 6160-6167.

**Stemple, D. L.** (2005). Structure and function of the notochord: an essential organ for chordate development. *Development* **132**, 2503-2512.

**Tukachinsky, H., Kuzmickas, R. P., Jao, C. Y., Liu, J. and Salic, A.** (2012). Dispatched and scube mediate the efficient secretion of the cholesterol-modified hedgehog ligand. *Cell Reports* **2**, 308-320.

**Westerfield, M.** (1995). *The Zebrafish Book*. Eugene, OR: University of Oregon Press.

**Woods, I. G. and Talbot, W. S.** (2005). The you gene encodes an EGF-CUB protein essential for Hedgehog signaling in zebrafish. *PLoS Biol.* **3**, e66.

**Yamamoto, M., Morita, R., Mizoguchi, T., Matsuo, H., Isoda, M., Ishitani, T., Chitnis, A. B., Matsumoto, K., Crump, J. G., Hozumi, K. et al.** (2010). Mib-Jag1-Notch signalling regulates patterning and structural roles of the notochord by controlling cell-fate decisions. *Development* **137**, 2527-2537.

**Yan, Y. L., Hatta, K., Riggleman, B. and Postlethwait, J. H.** (1995). Expression of a type II collagen gene in the zebrafish embryonic axis. *Dev. Dyn.* **203**, 363-376.

**Zhou, Y., Cashman, T. J., Nevis, K. R., Obregon, P., Carney, S. A., Liu, Y., Gu, A., Mosimann, C., Sondalle, S., Peterson, R. E. et al.** (2011). Latent TGF-β binding protein 3 identifies a second heart field in zebrafish. *Nature* **474**, 645-648.

**Supplementary Figure S1. Morpholino-mediated knockdown of zebrafish Emilin3 transcripts.** (**A**) RT-PCR analysis of RNA extracted from 24 hpf non-injected embryos (WT) and embryos injected with the indicated morpholinos. β-actin was used as a loading control. (**B**) Whole mount immunofluorescence labeling for Emilin3 in 24 hpf embryos injected with 4 ng control morpholino (Ctrl MO), 2 ng/each of *emilin3a* and *emilin3b* splice-blocking morpholinos (e3a+e3b MO splice), or 2 ng/each of *emilin3a* and *emilin3b* translation-blocking morpholinos (e3a+e3b MO ATG). Scale bar, 50 μm. (**C**) Lateral views of 24 hpf embryos injected with 4 ng control morpholino (Ctrl MO) or 2 ng/each of *emilin3a* and *emilin3b* translation-blocking morpholinos (e3a+e3b MO ATG). Arrows point at notochord distortions in Emilin3 double morphants. (**D**) Lateral views of 24 hpf embryos injected with 10 ng control morpholino (Ctrl MO), 2 ng/each of *emilin3a* and *emilin3b* splice-blocking morpholinos (e3a+e3b MO), 6 ng p53 translation-blocking morpholino (p53 MO) and the combination of p53, *emilin3a* and *emilin3b* morpholinos (e3a+e3b+p53 MO). no, notochord.

**Supplementary Figure S2. Quantification of the mean number of notochord cells.** (**A**) Notochord cell nuclei of the same trunk region from 24 hpf control and Emilin3 double morphant embryos were stained with Hoechst. Scale bar, 50 μm. (**B**) Nuclei, stained as in (A), were counted and reported as mean number of nuclei/somite (not significant; $n$=15). Ctrl MO, control morpholino; e3a+e3b MO, *emilin3a* + *emilin3b* morpholinos.

**Supplementary Figure S3. Notch activity is not grossly affected in the notochord of Emilin3 depleted embryos.** (**A**) Notch-responsive reporter zebrafish (Tg_Hbb:EGFP) were injected with the indicated morpholinos and the fluorescence analyzed at 24 hpf. Scale bar, 50 μm. (**B**) Quantification of the mean number of GFP-positive notochord cells in the trunk region (250 μm in length) (not significant; $n$=10). Ctrl MO, control morpholino; e3a+e3b MO, *emilin3a* + *emilin3b* morpholinos.

**Supplementary Figure S4. Analysis of collagen II and laminin expression in Emilin3 morphant embryos.** (**A**, **B**) Zebrafish embryos were injected with the indicated morpholinos and probed for *col2a1* expression at 24 and 48 hpf, respectively. The fraction of embryos displaying the corresponding phenotype is provided in each panel. Note that at 24 hpf, even embryos injected with *emilin3a* or *emilin3b* morpholino alone displayed a slight increase in *col2a1* expression. (**C**) Lateral views of controls and Emilin3 morphant embryos labeled by immunohistochemistry for laminin at 24 hpf. The panels display projection of confocal sections around somite 10, showing the notochord. Scale bar, 25 μm. Ctrl MO, control morpholino; e3a MO, *emilin3a* morpholino; e3b MO, *emilin3b* morpholino; e3a+e3b MO, *emilin3a* + *emilin3b* morpholinos.

**Supplementary Figure S5. Hedgehog upregulation in Emilin3 morphant embryos is dependent on Emilin3 protein depletion.** (**A, B**) Embryos were injected with the indicated splice- or translation-blocking morpholinos (ATG) and probed for *ptc1* expression at 24 hpf. Lateral view of the trunk, head is on the left. (**C**) Control and Emilin3 double morphant embryos were probed for *ptc1* expression at 8-somite stage. (**D**) Dorsal view of wild-type embryos immunostained for Emilin3 and β-catenin at at 8-somite stage. Note the absence of Emilin3 in the notochord (marked by the asterisks) at this stage of development. Scale bar, 100 μm. The fraction of embryos displaying the corresponding phenotype is provided in each panel. Ctrl MO, control morpholino; e3a+e3b MO, *emilin3a* + *emilin3b* morpholinos; p53 MO, p53 morpholino.

**Supplementary Figure S6. Upregulation of Hedgehog target genes in Emilin3 morphant embryos.** (**A**) Lateral views of 24 hpf embryos injected with the indicated morpholinos and probed for *olig2*, *vegfa* and *eng2a* expression. (**B**) Expression of *fgf8* is similar between control and Emilin3 double morphant embryos, thus excluding a generalized developmental delay. Head is on the left. The fraction of embryos displaying the corresponding phenotype is provided in each panel. Ctrl MO, control morpholino; e3a+e3b MO, *emilin3a* + *emilin3b* morpholinos.

**Supplementary Figure S7. Hedgehog upregulation in Emilin3 morphant embryos is not dependent on BMP or TGF-β signaling**. **(A**) Lateral views of 24 hpf embryos injected with the indicated morpholinos and treated at 8 hpf with 5 μM cyclopamine (lower panels) or with the corresponding volume of ethanol as a control (upper panels). Embryos were then stained with the monoclonal 4D9 antibody (green) and the polyclonal pSMAD1/5/8 antibody (purple). The panels show magnifications around somite 10. Scale bar, 50 μm. (**B**) Wild-type embryos were injected with the indicated morpholinos. Embryos were then left untreated or treated at 8 hpf with 30 μM of the selective TGF-β receptor inhibitor LY364947 from 8 hpf and probed for *ptc1* expression at 24 hpf. The fraction of embryos displaying the corresponding phenotype is provided in each panel. Ctrl MO, control morpholino; e3a+e3b MO, *emilin3a* + *emilin3b* morpholinos.

**Supplementary Figure S8. Injection of Emilin3 cDNA rescues the phenotype of Emilin3 morphants. (A)** Lateral views of 24 hpf embryos co-injected with the indicated morpholinos (4 ng/embryo) and with the indicated cDNA constructs (25 ng/μl). Arrows point at notochord distortions in Emilin3 double morphants, which are largely rescued by co-injection with the pCS-twhh-mEmilin3 construct. The fraction of embryos displaying the corresponding phenotype is provided in each panel. (**B**) Whole mount immunofluorescence labeling for engrailed and Emilin3 in 24 hpf embryos injected as in (A). Scale bar, 25 μm. (**C**) Quantification of engrailed-positive cells in 24 hpf co-injected embryos (*, $P < 0.05$; n.s., not significant; $n = 10$). Ctrl MO, control morpholino; e3a+e3b MO, *emilin3a* + *emilin3b* morpholinos; Trunk MPs, trunk muscle pioneers; Trunk MFFs, trunk medial fast fibers.

**Supplementary Figure S9**. **Conditioned medium from HEK293T cells can stimulate Shh release**. 293-Shh cells were incubated for 6 hr with fresh medium (DMEM) or with conditioned media derived from HEK293T transfected with the indicated plasmids. The release rate of Shh was assessed by immunoblot of media and cell lysates. CM, conditioned media; E3, murine full-length Emilin3; ev, empty vector; WB, western blot.

**Supplementary Figure S10. Emilin3 and Scube2 functionally interact.** (**A**) Cell lysates of HEK293T transfected with the indicated plasmids were either analyzed directly by western blot or subjected to immunoprecipitation with an anti-HA affinity gel followed by western blot for Scube2 (anti-FLAG). (**B**) *In vitro* binding between Emilin3 and the EGF fragment of Scube2. HEK293T were transiently co-transfected with Emilin3 or Scube2-EGF constructs. Media were then harvested, and subjected to western blot and immunoprecipitation with the indicated antibodies. (**C**) HEK293T were co-transfected with the Shh plasmid and the indicated constructs and left untreated or treated overnight with 50 μg/ml of soluble heparin in serum free medium. Cell lysates and conditioned media were then analyzed by immunoblotting. (**D**,**E**) HEK293T were co-transfected with the Shh plasmid and the indicated constructs (D) or transfected and then treated with increasing concentration of Scube2-conditioned medium (E). Shh release was then studied by western blot. E3, murine full-length Emilin3 cDNA; E3-HA, murine full-length HA-tagged Emilin3 cDNA; ev, empty vector; IP, immunoprecipitation; Scube2-FLAG, murine full-length FLAG-tagged Scube2 cDNA; WB, western blot.

**Supplementary Figure S11. Morpholino-mediated knockdown of zebrafish Emilin3 and Scube2.** (**A**) Lateral views of 24 hpf embryos injected with 6 ng of control morpholino (Ctrl MO) or 2 ng/each of the indicated morpholinos. (**B**) qRT-PCR for *scube2* transcript in control and Emilin3 double morphant embryos (not significant; $n = 30$). Ctrl MO, control morpholino; e3a+e3b MO, *emilin3a* + *emilin3b* morpholinos; Scube2 MO, Scube2 morpholino.

**Supplementary Table S1. Summary of the phenotypic defects detected after injection of morpholino oligonucleotides.** Wild-type zebrafish embryos were injected with the indicated morpholinos and examined at 24 hpf. The dose for each morpholino, the total number of injected embryos, and the number and percentage of embryos displaying the indicated phenotypic defects is provided. Embryos were assigned to one of the following three classes based on their phenotype: *a)* normal (no evidence of morphological defect); *b)* notochord defects; *c)* radialized embryos. Ctrl, control morpholino; e3a splice, *emilin3a* splicing-blocking morpholino; e3b splice, *emilin3b* splicing-blocking morpholino; e3a ATG, *emilin3a* translation-blocking morpholino; e3b ATG, *emilin3b* translation-blocking morpholino.

**Supplementary Table S2. Sequences of morpholino oligonucleotides used in the study.** The table describes the sequences of morpholinos targeting the donor splice site between the first exon and the first intron of *emilin3a* or *emilin3b* (e3a MO splice and e3b MO splice), the splice site between the first exon and the first intron of *col2a1* (col2a1 MO splice; Mangos et al., 2010), the translation initiation codon of *emilin3a* or *emilin3b* (e3a MO ATG and e3b MO ATG), the translational initiation codon of *scube2* (scube2 MO ATG; Woods et al., 2005), the translation initiation codon of p53 (p53 MO ATG; Robu et al., 2007) and a standard control morpholino (Ctrl MO). All sequences were provided by Gene tools, LLC.

# Figure S1

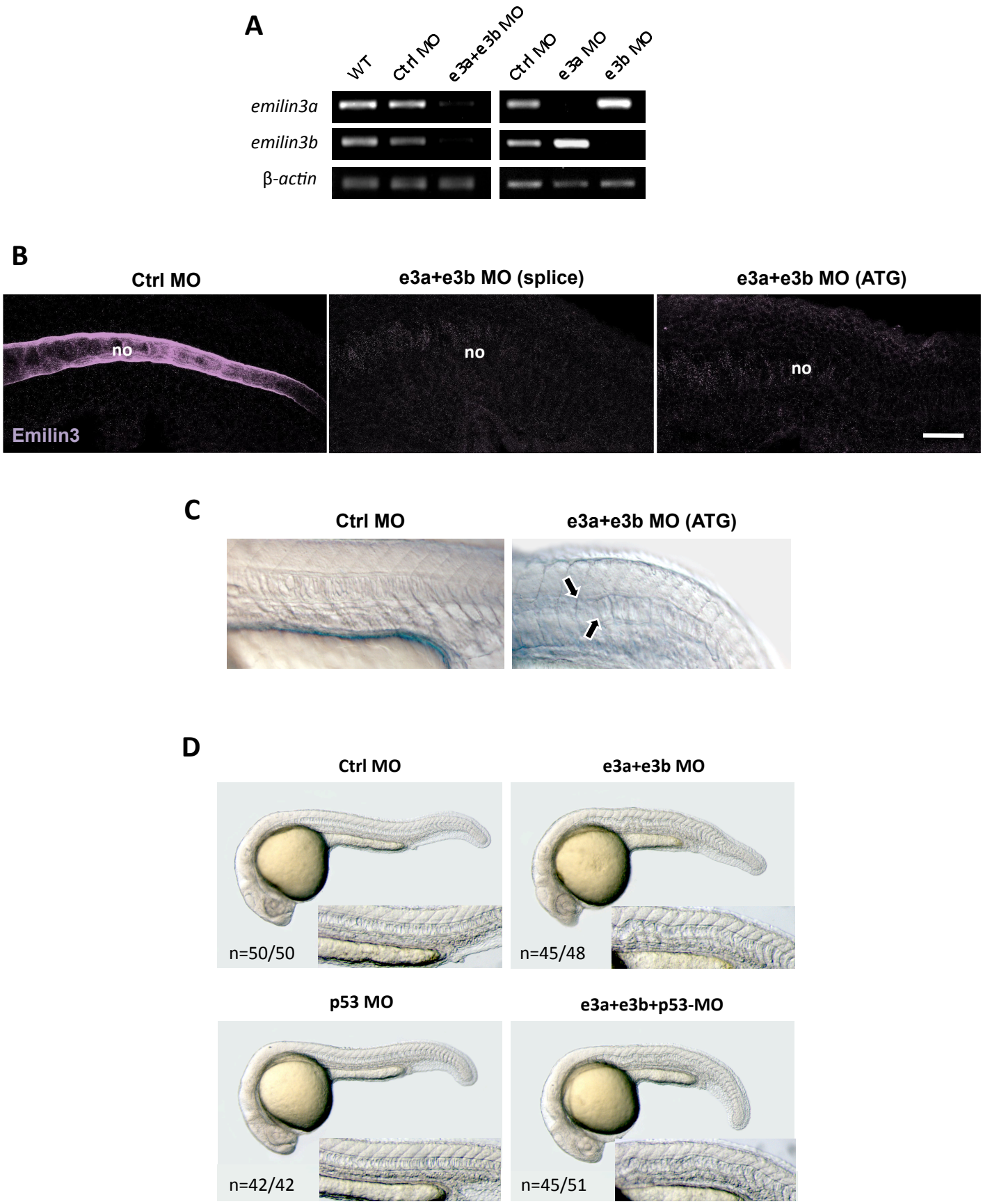
A
WT
Ctrl MO
e3a+e3b MO
Ctrl MO
e3a MO
e3b MO
emilin3a
emilin3b
β-actin
B
Ctrl MO
e3a+e3b MO (splice)
e3a+e3b MO (ATG)
no
no
no
Emilin3
C
Ctrl MO
e3a+e3b MO (ATG)
D
Ctrl MO
e3a+e3b MO
n=50/50
n=45/48
p53 MO
e3a+e3b+p53-MO
n=42/42
n=45/51

# Figure S2

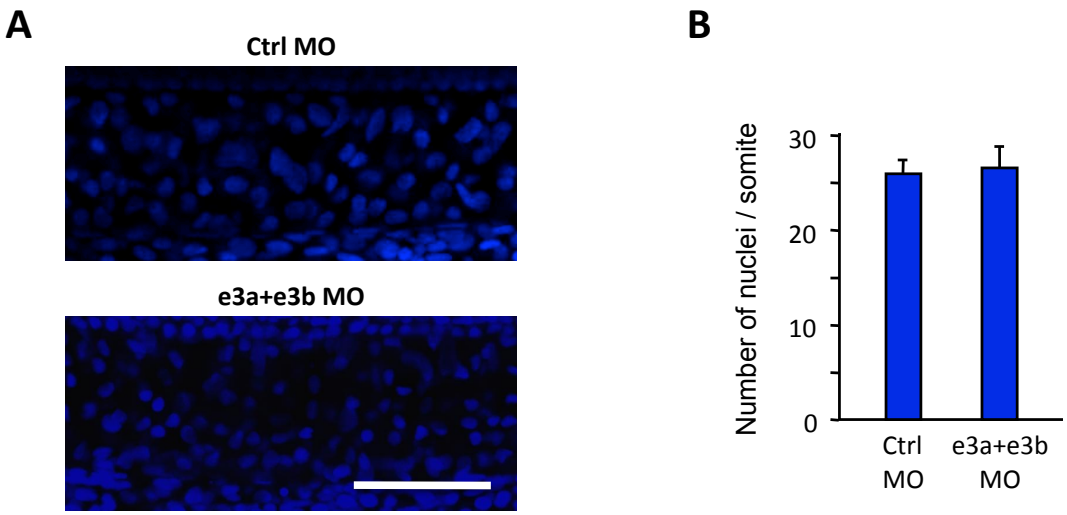
A
Ctrl MO
e3a+e3b MO
B
Number of nuclei / somite
30
20
10
0
Ctrl MO
e3a+e3b MO

# Figure S3

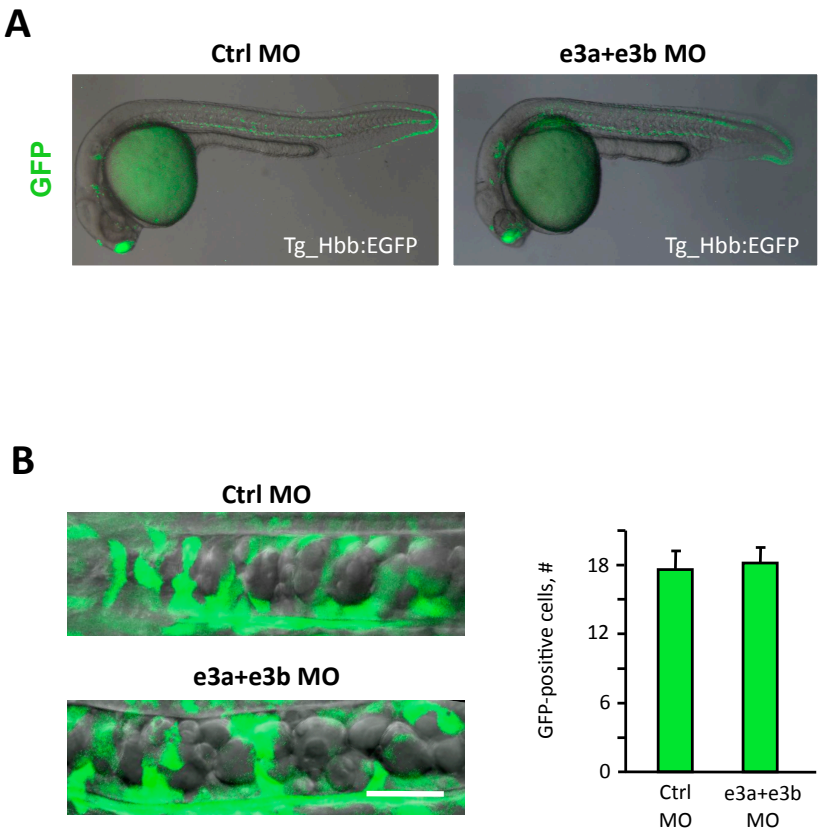
A
Ctrl MO
e3a+e3b MO
GFP
Tg_Hbb:EGFP
Tg_Hbb:EGFP
B
Ctrl MO
e3a+e3b MO
GFP-positive cells, #
18
12
6
0
Ctrl MO
e3a+e3b MO

# Figure S4

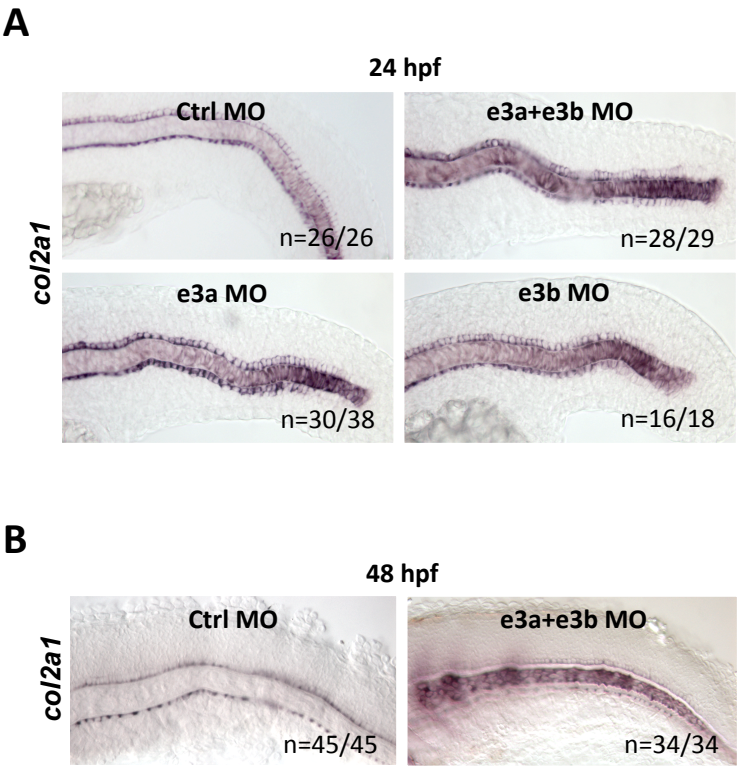
A
24 hpf
col2a1
Ctrl MO
n=26/26
e3a+e3b MO
n=28/29
e3a MO
n=30/38
e3b MO
n=16/18
B
48 hpf
col2a1
Ctrl MO
n=45/45
e3a+e3b MO
n=34/34

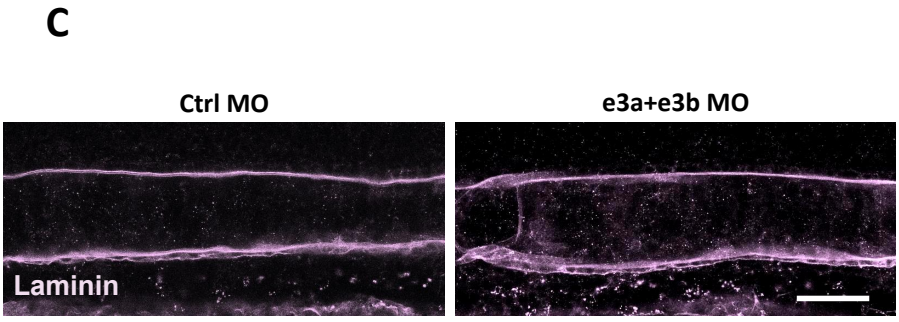
C
Ctrl MO
e3a+e3b MO
Laminin

# Figure S5

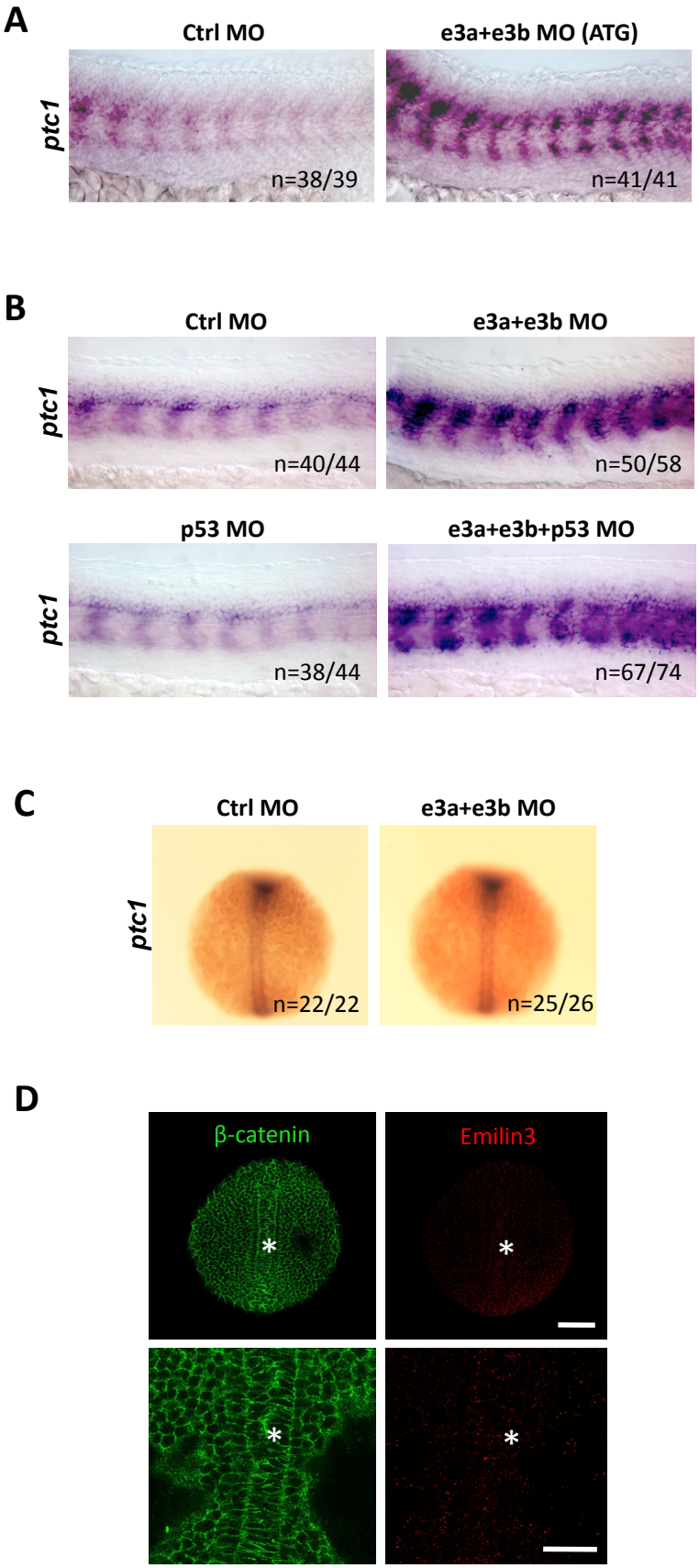
A
Ctrl MO
e3a+e3b MO (ATG)
ptc1
n=38/39
n=41/41
B
Ctrl MO
e3a+e3b MO
ptc1
n=40/44
n=50/58
p53 MO
e3a+e3b+p53 MO
ptc1
n=38/44
n=67/74
C
Ctrl MO
e3a+e3b MO
ptc1
n=22/22
n=25/26
D
β-catenin
Emilin3

# Figure S6

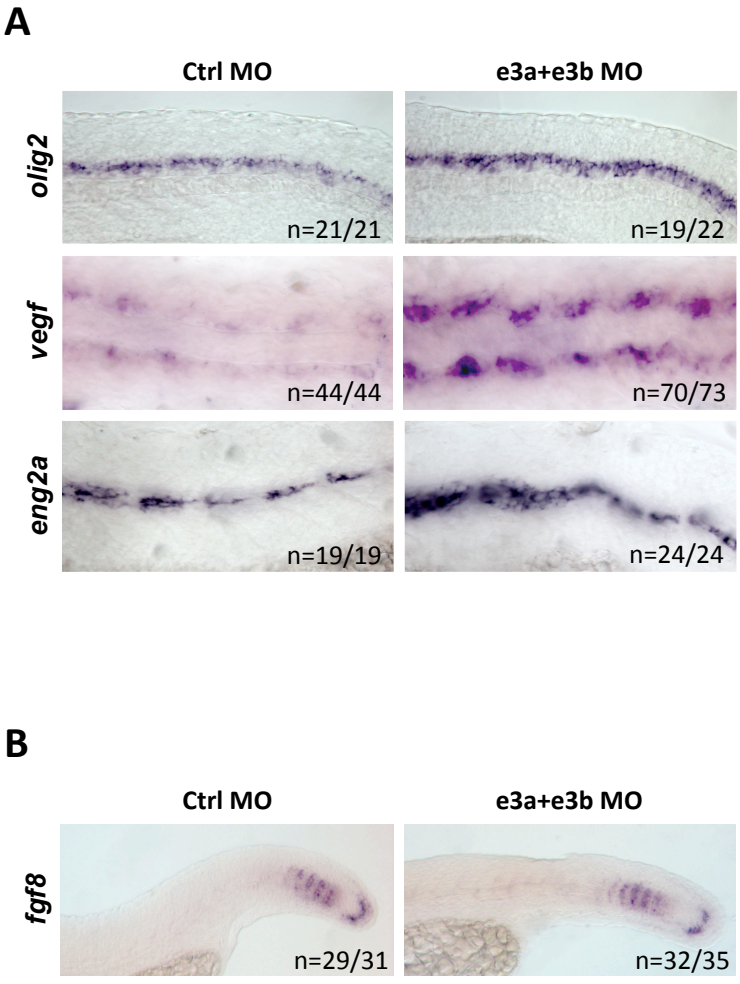
A
Ctrl MO
e3a+e3b MO
olig2
n=21/21
n=19/22
vegf
n=44/44
n=70/73
eng2a
n=19/19
n=24/24
B
Ctrl MO
e3a+e3b MO
fgf8
n=29/31
n=32/35

# Figure S7

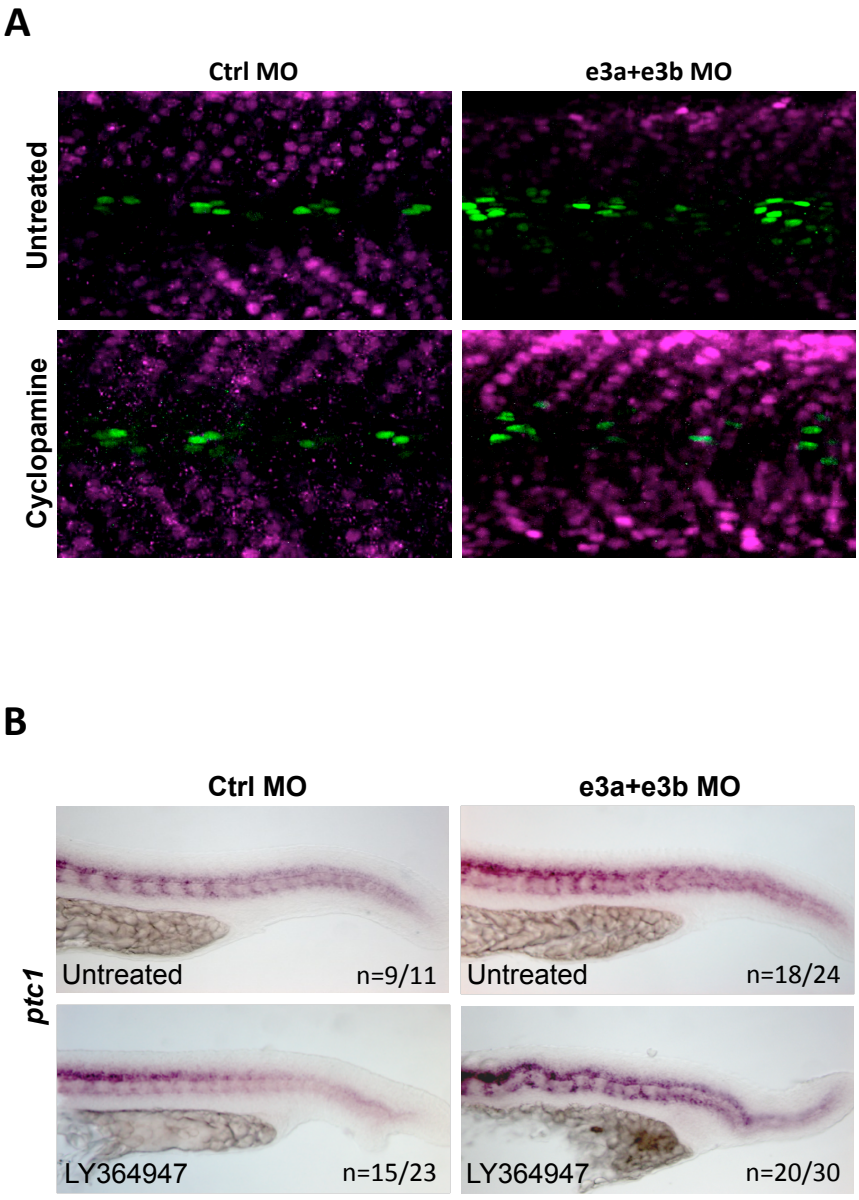
A
Ctrl MO
e3a+e3b MO
Untreated
Cyclopamine
B
Ctrl MO
e3a+e3b MO
ptc1
Untreated
n=9/11
Untreated
n=18/24
LY364947
n=15/23
LY364947
n=20/30

# Figure S8

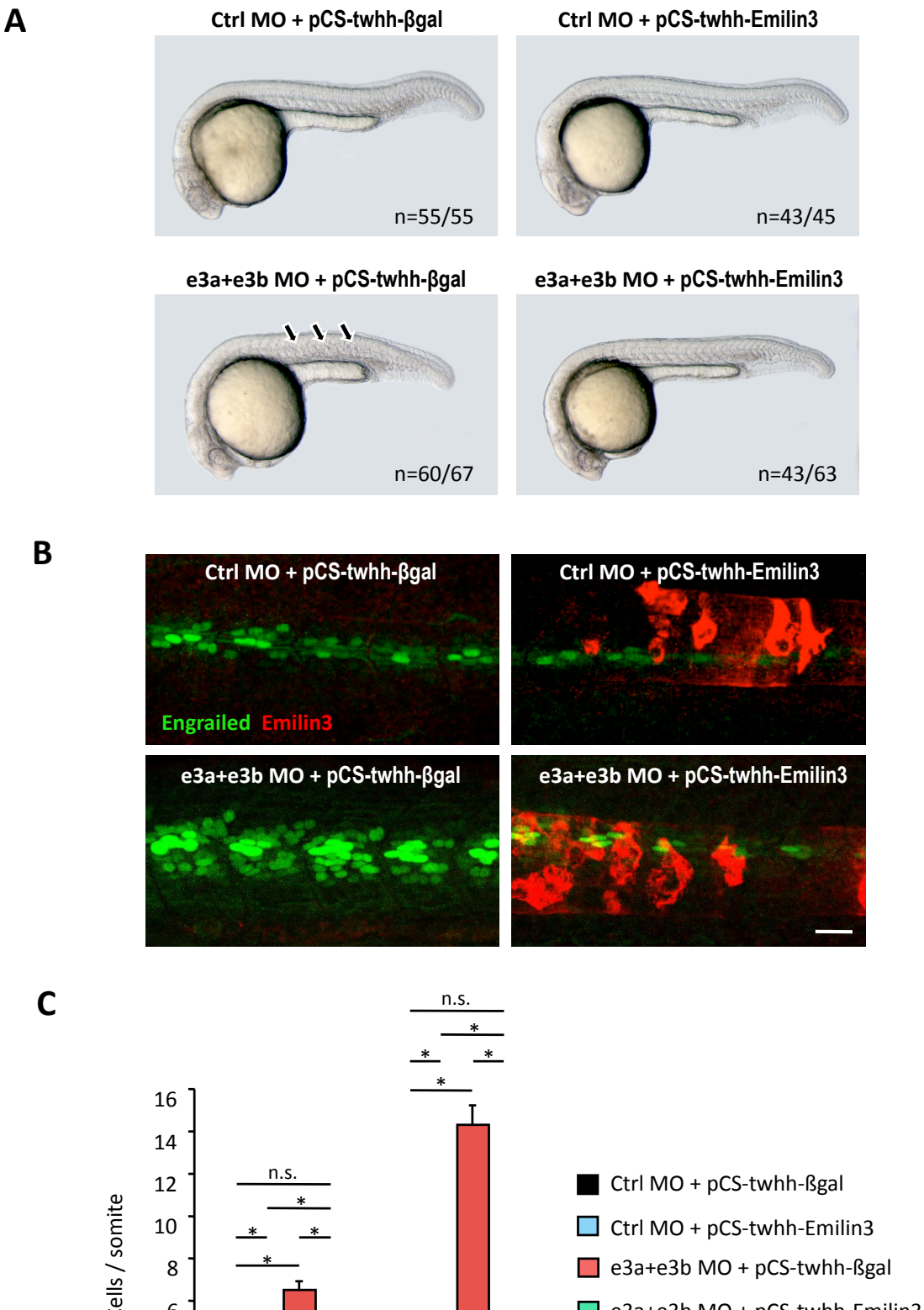
A
Ctrl MO + pCS-twhh-βgal
n=55/55
Ctrl MO + pCS-twhh-Emilin3
n=43/45
e3a+e3b MO + pCS-twhh-βgal
n=60/67
e3a+e3b MO + pCS-twhh-Emilin3
n=43/63
B
Ctrl MO + pCS-twhh-βgal
Engrailed Emilin3
Ctrl MO + pCS-twhh-Emilin3
e3a+e3b MO + pCS-twhh-βgal
e3a+e3b MO + pCS-twhh-Emilin3
C
Cells / somite
16
14
12
10
8
6
4
2
0
n.s.
*
*
*
*
n.s.
*
*
*
*
Trunk MPs
Trunk MFFs
Ctrl MO + pCS-twhh-ßgal
Ctrl MO + pCS-twhh-Emilin3
e3a+e3b MO + pCS-twhh-ßgal
e3a+e3b MO + pCS-twhh-Emilin3

# Figure S9

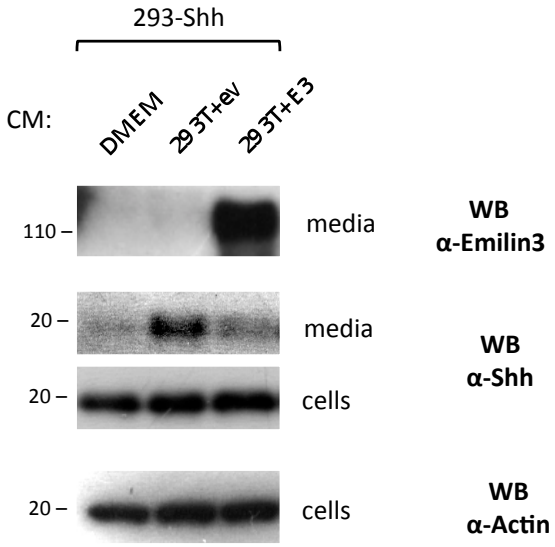
293-Shh
CM:
DMEM
293T+ev
293T+E3
110 –
media
WB
α-Emilin3
20 –
media
20 –
cells
WB
α-Shh
20 –
cells
WB
α-Actin

# Figure S10

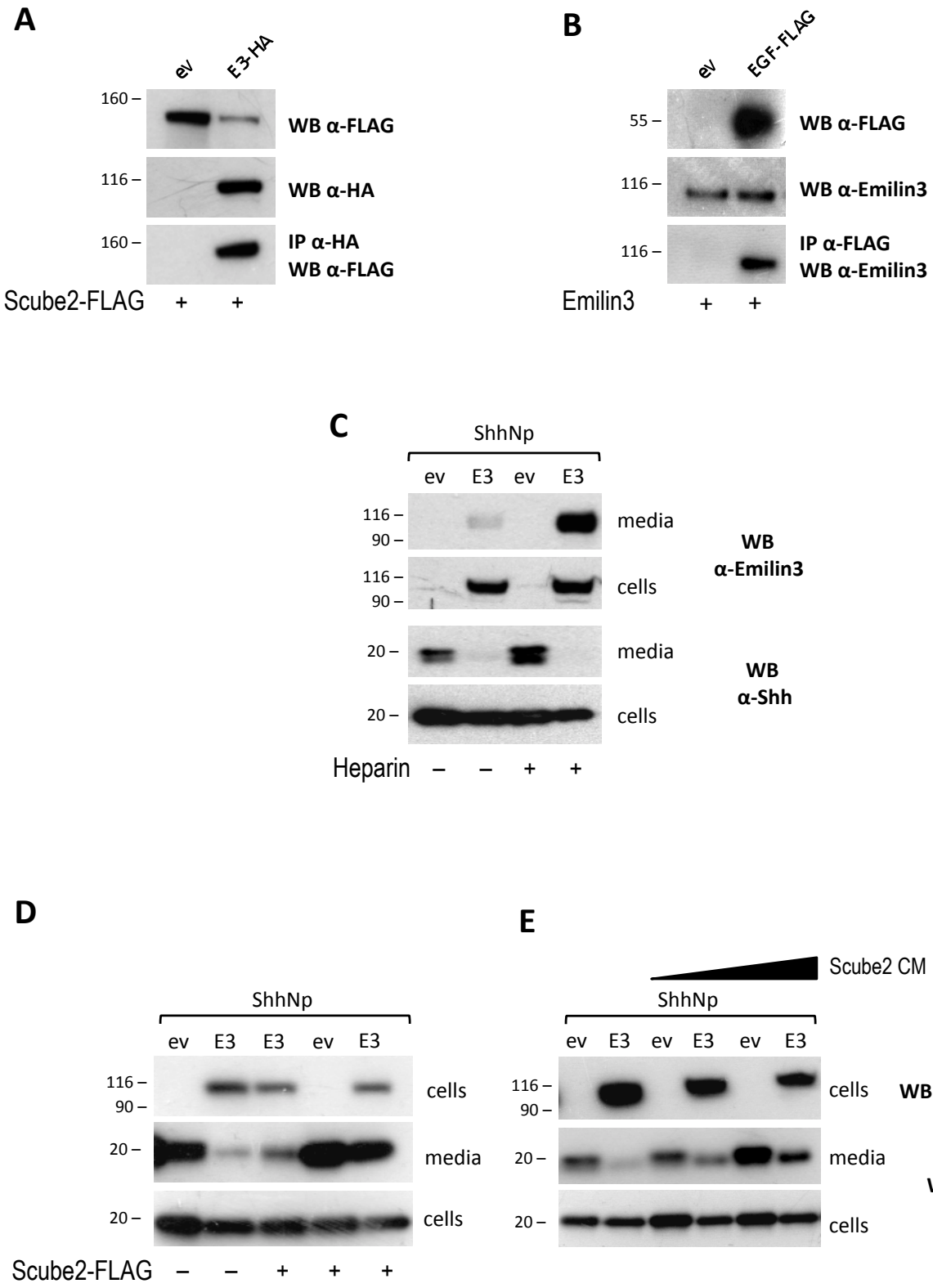
A
ev
E3-HA
160 –
WB α-FLAG
116 –
WB α-HA
160 –
IP α-HA
WB α-FLAG
Scube2-FLAG + +
B
ev
EGF-FLAG
55 –
WB α-FLAG
116 –
WB α-Emilin3
116 –
IP α-FLAG
WB α-Emilin3
Emilin3 + +
C
ShhNp
ev E3 ev E3
116 –
90 –
media
116 –
90 –
cells
WB
α-Emilin3
20 –
media
20 –
cells
WB
α-Shh
Heparin – – + +
D
ShhNp
ev E3 E3 ev E3
116 –
90 –
cells
20 –
media
20 –
cells
Scube2-FLAG – – + + +
E
Scube2 CM
ShhNp
ev E3 ev E3 ev E3
116 –
90 –
cells
WB α-Emilin3
20 –
media
WB α-Shh
20 –
cells

# Figure S11

**A**


**B**

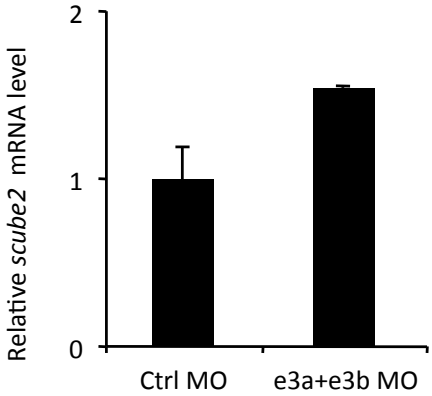

# Table S1

| Type of morpholino | Dose (ng) | Embryos examined | Phenotype | | |
|---|---|---|---|---|---|
| | | | Normal | Notochord defects | Radialized embryos |
| Ctrl | 4 | 153 | 151 (99%) | 0 (0%) | 2 (1%) |
| e3a (splice) | 2 | 63 | 61 (97%) | 1 (1.5%) | 1 (1.5%) |
| e3a (splice) | 4 | 68 | 50 (74%) | 17 (25%) | 1 (1%) |
| e3b (splice) | 2 | 63 | 58 (92%) | 3 (5%) | 2 (3%) |
| e3b (splice) | 4 | 63 | 54 (86%) | 7 (11%) | 2 (3%) |
| e3a (splice) + e3b (splice) | 4 + 4 | 80 | 3 (5%) | 58 (92%) | 2 (3%) |
| | 2 + 2 | 231 | 33 (14%) | 195 (84%) | 3 (2%) |
| | 0.5 + 0.5 | 55 | 61 (97%) | 1 (1.5%) | 1 (1.5%) |
| e3a (ATG) | 2 | 69 | 51 (74%) | 17 (24%) | 1 (2%) |
| e3b (ATG) | 2 | 51 | 38 (75%) | 13 (25%) | 0 (0%) |
| e3a (ATG) + e3b (ATG) | 2 + 2 | 106 | 12 (11%) | 94 (89%) | 0 (0%) |
| Ctrl | 3.5 | 40 | 37 (92%) | 0 (0%) | 3 (8%) |
| e3a (splice) | 2 | 63 | 61 (97%) | 1 (1.5%) | 1 (1.5%) |
| e3b (ATG) | 1.5 | 42 | 42 (100%) | 0 (0%) | 0 (0%) |
| e3a (splice) + e3b (ATG) | 2 + 1.5 | 62 | 27 (44%) | 33 (53%) | 2 (3%) |

# Table S2

| Type of morpholino | Sequence |
|---|---|
| e3a MO (splice) | 5’ –TTACTCATGGATACTTACTTGTGCC– 3’ |
| e3b MO (splice) | 5’ –TAGCGTTTACTTACTTATGATGCCC– 3’ |
| col2a1 MO (splice) | 5’ –TGAAAAACTCCAACTTACGGTCATC– 3’ |
| e3a MO (ATG) | 5’ –TGCAAAATCTTCTCC AGTAGCATGA– 3’ |
| e3b MO (ATG) | 5’ –ACGGAAATGCAAGAATCCACCTCAT– 3’ |
| scube2 MO (ATG) | 5’ –GCCGTACAGTCCAAACAGCTCCCAT– 3’ |
| p53 MO (ATG) | 5’ –GCGCCATTGCTTTGCAAGAATTG– 3’ |
| Ctrl MO | 5’ –CCTCTTACCCTAGTTACAATTTATA– 3’ |